Stimulation and Recording of Neural Tissue, Closing the Loop on the Artifact

(Invited Paper)

Edgar A. Brown*, James D. Ross*, Richard A. Blum* and Stephen P. DeWeerth[†]

*School of Electrical and Computer Engineering
Georgia Institute of Technology. Atlanta, Georgia.
Emails: edgar.brown@gatech.edu, jross@neuro.gatech.edu, richard.a.blum@gatech.edu
[†]School of Electrical and Computer Engineering. Georgia Institute of Technology
and Emory University School of Medicine. Atlanta, Georgia.
Email: steve.deweerth@gatech.edu

Abstract—**To achieve the full potential of neural prostheses, such as those used for the treatment of epilepsy, some means to close the loop around the electrical stimulation protocol has to be provided. To be able to close the loop, it is necessary to record the effect of stimulation itself on the surrounding tissue. Such recording is made impossible by the presence of a long-lasting stimulation artifact, which is due to the presence of residual charge in the electrode. Custom electronics, implementing a novel feedback scheme, can reduce or eliminate such charge and, by making the electronics scalable, a large number of electrodes can be simultaneously accessed. In this work we present such an artifact elimination system.**

I. Introduction

Clinical use of electrical stimulation of tissue has a story that spans more than 50 years, from its routine use in cardiac pacemakers [1], [2] to the more recent neural prostheses (NPs) that electrically activate central and peripheral neural systems [3], [4]. NPs in particular have shown significant promise in supplementing function lost to disease or injury, from restoring hearing [5] to the control of upper and lower extremities [6], [7]. One of the advancing areas in NPs is in the direct stimulation of the brain. Deep brain stimulation (DBS) prostheses, as these are called, have shown their usefulness in treating the tremors associated with Parkinson's disease and multiple sclerosis [8], and the seizures of epilepsy [9].

All existing NPs, however, seek to overpower the underlying neural mechanisms instead of modulating them to achieve the desired outcome. This is particularly true for DBS, in which brain-implanted electrodes emulate a brain lesion, for the treatment of Parkinson's disease, multiple sclerosis, or epilepsy [8]. Though this is more agreeable than the alternative of physically removing large sections of the brain, in the case of epilepsy the procedure still fails for a large percentage of seizures [10], [11]. A basic limitation to achieve a finer degree of control is the impossibility to react, in real time, to the neural response to a stimulus. This limitation results from the impossibility to record after applying an electrical stimulus, which is due to the stimulation artifact.

The stimulation artifact has troubled electrophysiologists since early stimulation experiments. Its presence obscures the recording of neural activity near the stimulation site for tens
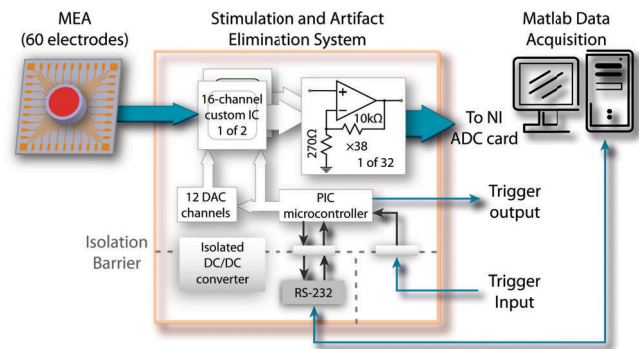

Figure 1. Artifact elimination testing system. A multi-electrode array (MEA) is connected by means of a Multi Channel Systems (MCS) preamplifier plate (being used passively as an interface). The AD Board is a National Instruments 6035E, connected to the specific channels under test. An RS-232 (serial) interface is used to program the stimulation and artifact elimination parameters. Trigger signals from the custom board are used to synchronize data acquisition and stimulus generation.

or hundreds of milliseconds [12], eliminating any possibility to directly assess the result of a stimulus. Although several investigators have tried to cancel the artifact after it has occurred [13], [14], and some groups have tried to eliminate it at its source [15], [16], there is still little understanding of the artifact process and properties.

In the present work we describe a stimulation, recording, and artifact elimination system (Fig. 1). Our artifact elimination system is built around an IC described in [17], which directly manipulates the source of the artifact—the electrode charge—using a novel feedback scheme.

II. Eliminating the Stimulation Artifact

To completely describe the stimulation artifact, further investigation is required. We have found, however, that a linear RC model of the electrode is all that's needed to sufficiently describe the artifact problem. With the right circuitry, such RC model is also enough to significantly reduce the stimulation artifact.

1) Artifact origin: The stimulation artifact is a direct consequence of the accumulated charge in the electrode–electrolyte
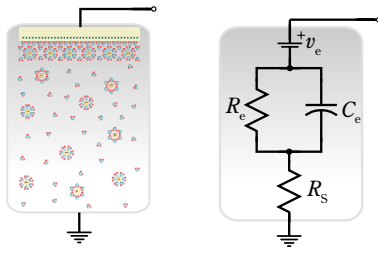
Figure 2. Simplified electrode model. When a metal is submerged in a solution, solvated ions and water molecules form a layer that surrounds the metal. The simplest model of this contact layer is shown; it comprises v_e the electrochemical potential, C_e the electrode capacitance, and R_e the electrode resistance (R_e and C_e depend on the electrode–electrolyte contact area). R_S, the spreading resistance, models the resistance of the solution itself (and depends on the geometrical area of the electrode).

interface during stimulation and of the effect that this charge has on the signal-chain filters and other elements after stimulation [18]. The problem is one of relative scales: stimulation signals are on the order of hundreds of millivolts (or more), while recorded signals are on the order of tens of microvolts. Even if charge balancing is made part of the stimulation protocol, small mismatches, that are common and acceptable in traditional designs, generate artifacts that would saturate the signal acquisition chain. The problem is further complicated by the redox (reduction/oxidation) reactions that take place at the electrode–electrolyte interface and by electrode surface roughness effects (constant-phase electrode response), both of which make charge balancing difficult to accomplish. If no attempt at charge balancing is made, such saturation would be even more pronounced and longer lasting.

The stimulation artifact can be understood through the RC model of Fig. 2. After stimulation, an open electrode would have to discharge its capacitance (C_e) through R_e, resulting in a time constant of $R_e \times C_e$. For a $40 \, \mu m \times 40 \, \mu m$ platinum black extracellular electrode, this would result in a $10 \, ms$ time constant. For typical stimulation protocols, in which a residual voltage of $200 \, mV$ or more can be left in the electrode, to bring the charge to a level that lies within the recording range of the circuitry (around $2 \, mV$ in many cases) five time constants (i.e., $\ln \left[200 \, mV / 2 \, mV \right]$) would have to elapse. Given that neurons respond within $20 \, ms$ or less to such stimulation, no direct recording of the initial neural response would be possible.

2) Artifact elimination: By connecting the electrode through a low impedance path to an *appropriate voltage*, we can reduce the time constant from the $10 \, ms$ of the previous section to approximately $200 \, \mu s$ ($R_S C_e$ in Fig. 2, for polarizable electrodes $R_e \gg R_S$), a 50-fold reduction. Such reduction should allow recording within $1 \, ms$ of the stimulus, enabling the recording of the initial stimulation response. Given that the electrode is non-linear (and non-stationary), two problems remain with this approach: 1) the time constants can change as the electrode discharges, and 2) we have to determine what is an appropriate voltage.'

One way to design around these problems is to incorporate a feedback loop around the electrode. By designing this
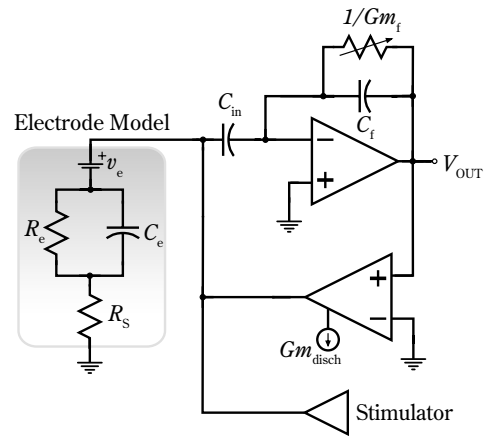

Figure 3. IC electrode-interface circuitry, notice that the main amplifier is part of the discharge loop and it is responsible for storing the electrode DC voltage. Gm_{disch} is the transconductance (bias) of the discharge amplifier, G_{m_f} the transconductance (bias) of a $G_m C$ stage (which sets the high-pass pole frequency). All the amplifiers can be independently turned on and off through switch transistors in the tail current of their input differential pairs; as any switches in the signal path (and their charge injection) are very undesirable given the required amplification.
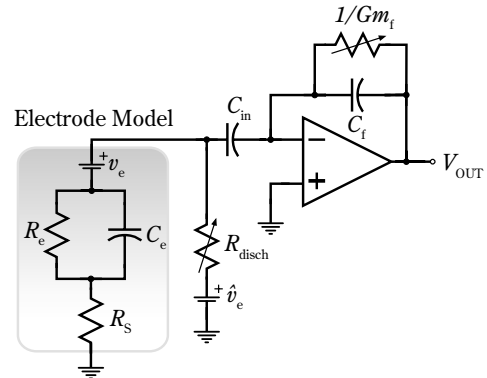

Figure 4. Equivalent discharge circuitry disregarding the frequency response and saturation characteristics of the amplifiers. $\hat{v}_e$ is the low-pass estimate of the electrochemical potential.

feedback loop such that it has a stable point at the discharged electrode condition, and if the loop remains stable during the discharge process, we can reduce dependency on the many unknown electrode factors. Furthermore, by turning the feedback elements on and off, we can remove the need for additional switches (and their charge injection). For lack of a better approximation, our initial approach is to assume that the appropriate voltage' is the electrode average voltage before stimulation.

3) Artifact elimination circuitry: A high-level schematic of our circuitry can be seen in Fig. 3 [19]. The capacitive feedback, combined with a feedback OTA, sets the gain and high-pass pole of the amplifier (see [17]). The discharge amplifier is a basic OTA stage biased for sub-threshold operation. During normal operation, with the discharge amplifier turned off, the capacitive components of the main amplifier will store the average electrode voltage; this is a consequence of the

357

zero at $0\,\text{Hz}$ from the high-pass configuration. Activating the discharge amplifier will force the output of the main amplifier to zero, which in turn will force the electrode node to the stored average voltage. Assuming that all amplifiers are in linear range (and ignoring their frequency characteristics), the discharge regime can be represented by the circuit in Fig. 4. During the discharge phase the circuitry is roughly equivalent to connecting the electrode, through a controllable resistor given by

$$R_{\text{disch}} \approx \frac{1}{A_{\text{V}} G_{\text{m}_{\text{disch}}}} = \frac{U_{\text{T}}}{A_{\text{V}} I_{\text{disch}}} \qquad (1)$$

to the pre-stimulation average electrode DC voltage (where $A_{\text{V}} \approx 200$ is the main amplifier gain, $U_{\text{T}} \approx 26\,\text{mV}$ the thermal voltage, and I_{disch} the discharge amplifier bias current). Although a direct galvanic connection to the electrode is employed in this work, as is common use for neural research instrumentation, this scheme would also work with capacitive coupling to the electrode, a necessity in human implants.

Table I
CIRCUIT SPECIFICATIONS

Parameter	Value
Main amplifier bias	$25\,\mu\text{A}$
Main amplifier voltage gain	200
Main amplifier high-pass	$2\,\text{Hz}\text{-}300\,\text{Hz}$
Main amplifier low-pass	$3.3\,\text{kHz}$
$C_{\text{I}}/C_{\text{F}}$	$8\,\text{pF}/40\,\text{fF}$
Input referred noise ($200\,\text{Hz}\text{-}3\,\text{kHz}$)	$3\,\mu\text{V}_{\text{RMS}}$
Maximum stimulation current	$\pm 100\,\mu\text{A}$
Maximum stimulation voltage	$\pm 1.3\,\text{V}$
Circuit area ($0.35\,\mu\text{m}$ technology)	$0.05\,\text{mm}^2$

III. RESULTS

To test our circuitry, we used $40\,\mu\text{m}$ commercial gold electrodes (Ayanda Biosystems). Platinum black electroplating was used to equalize electrode impedances, bringing all electrodes to approximately $20\,\text{k}\Omega$ at $1\,\text{kHz}$ ($C_{\text{e}} \approx 15\,\text{nF}$, $R_{\text{S}} \approx 10\,\text{k}\Omega$). We submerged the electrodes in a saline medium that emulates *in vivo* conditions (Hank's Balanced Salt Solution, Hyclone), and placed an additional wire in the media to provide a low-impedance ground connection. Although linear stability analysis predicts unconditional stability under our discharge conditions [17], very brief decaying oscillations were observed with some electrodes.

Fig. 5 shows the behavior of the artifact elimination circuitry under a $+0.5\,\text{V}$ $250\,\mu\text{s}$ followed by $-0.5\,\text{V}$ $150\,\mu\text{s}$ stimulus. This stimulus asymmetry was used to improve charge balance, under this condition the undischarged artifact saturates the recording system for more than $15\,\text{ms}$ (with the external amplifier gain set to 1, this setup saturates above $6\,\text{mV}$). The ringing in the recording is independent of the artifact and is a consequence of the external buffer amplifier of our test setup. The initial spike in the recording occurs when the main amplifier and the discharge amplifier are turned on, during this
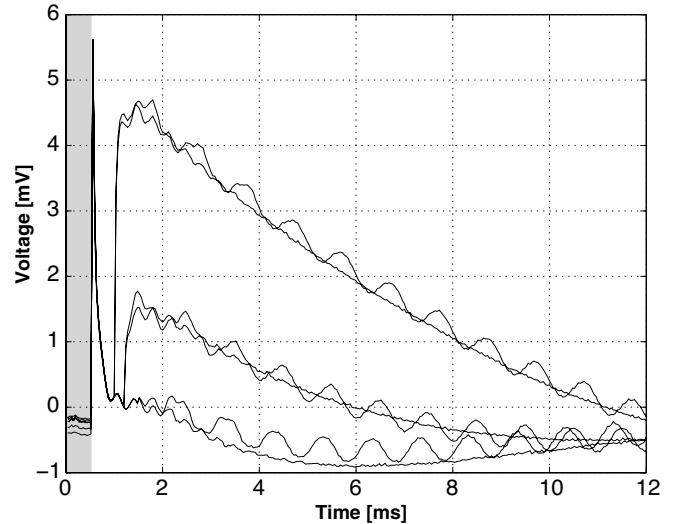

Figure 5. Effect of the artifact-elimination circuitry. The curves shown are for discharge durations of 0.5, 0.7, and $1.0\,\text{ms}$. Two sets are shown: with and without a $500\,\mu\text{V}_{\text{peak}}$, $1\,\text{KHz}$ sine wave applied to the saline solution (to emulate recording conditions). During stimulation the recording amplifier is deactivated (shaded interval). After stimulation, the artifact-elimination circuitry allows for the observation of the sine wave within $2\,\text{ms}$. From [17].
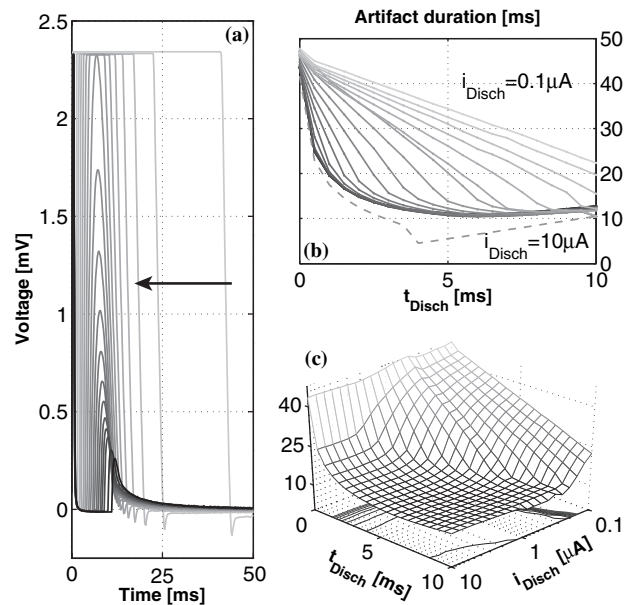

Figure 6. Artifact duration after a $\pm 0.5\,\text{V}$, $200\,\mu\text{s}$ per phase stimulus, and an initial discharge period of $500\,\mu\text{s}$ at $10\,\mu\text{A}$. The duration is measured as the time it takes to return to $200\,\mu\text{V}$ from the electrode voltage before the stimulus. (a) Set of time traces of artifact data with a discharge current of $10\,\mu\text{A}$ parameterized by discharge time, the arrow indicates the direction of increasing discharge time. (b) Artifact duration with respect to discharge time parameterized by discharge current (logarithmically spaced, 20 current traces from $10\,\mu\text{A}$ to $0.1\,\mu\text{A}$). The dashed line corresponds to a higher artifact threshold of $2\,\text{mV}$ (the sloped region is the total discharge time as the artifact does not exceed the threshold). (c) 3-D representation of the data set from (b). Note that the artifact duration slightly worsens for larger discharge currents and times. From [20].

358

interval the discharge is slew-rate limited by the current of the discharge amplifier.

Fig. 6 shows the control the discharge loop exerts on the artifact. To better visualize the artifact behavior, an initial discharge period of $500\,\mu s$ at $10\,\mu A$ has been used. Under the $\pm 0.5\,V$, $200\,\mu s$ per phase stimulus conditions, an undischarged electrode would saturate the recording system for $100\,ms$ (in this case the overall gain, with the external amplifier, was 3200). We have defined artifact duration as the time from the end of the stimulus to the point that the electrode returns to $200\,\mu V$ from the electrode voltage just before the stimulus. To reduce the influence of electrode transients, after every parameter change 25 stimulation cycles were thrown away and the last five cycles were captured and averaged; stimulation was kept at a fixed $8\,Hz$ rate. Additional long artifact elimination cycles were used in between parameter changes to reduce the chance of electrode damage during testing (which we have observed with this form of stimulation). The 420 data points in Fig. 6 encompass 2100 artifacts, extracted from more than 13000 stimulation and artifact cancellation cycles.

IV. CONCLUSIONS

We have presented a scalable custom IC that enables recording within $2\,ms$ of the stimulus on a stimulating channel. Our circuit achieves artifact elimination by directly discharging the electrode through a novel feedback scheme. This approach represents a break from existing artifact reduction methods; with our circuit we prevent the artifact problem instead of fighting its consequences. We have also shown that our approach can bring the artifact, traditionally regarded as unpredictable, under the control of known parameters in a simple linear model. This system represents a necessary first step to allow the direct closing of the loop around neural stimulation.

The main discharge speed limitation in our system is still given by the electrode impedance characteristics. Although the current performance might be enough for many applications, we have realized that we have not yet achieved the fastest discharge time possible (even under the RC electrode model). To further reduce the discharge time, it is necessary to reduce the RC constant of the electrode. This can be done by implementing a negative discharge impedance, which would reduce the effect of R_S on the time constant. Additionally, the electrode can display very long lasting transients (up to several seconds) that deviate from the assumption of the electrode returning to its pre-stimulation potential. These transients contribute to the artifact and its variability. If the discharge feedback loop required the electrode current to become zero, the electrochemical potential could then remain a free parameter. We are implementing both modifications (negative impedance and current zeroing) into our feedback scheme, which should consistently reduce the artifact to less than $1\,ms$.

REFERENCES

[1] B. Luderitz, "We have come a long way with device therapy: historical perspectives on antiarrhythmic electrotherapy." *J Cardiovasc Electrophysiol*, vol. 13, no. 1 Suppl, pp. S2–8, 2002.

[2] N. Klein, M. Klein, A. Salameh, and D. Pfeiffer, "[modern pacing therapy]," *Internist (Berl)*, vol. 47, no. 10, pp. 1024, 1026–30, 1032–3, 2006.

[3] A. Prochazka, V. K. Mushahwar, and D. B. McCreery, "Neural prostheses." *J Physiol*, vol. 533, no. Pt 1, pp. 99–109, 2001.

[4] R. B. Stein and V. Mushahwar, "Reanimating limbs after injury or disease." *Trends Neurosci*, vol. 28, no. 10, pp. 518–524, 2005.

[5] F. A. Spelman, "The past, present, and future of cochlear prostheses." *IEEE Eng Med Biol Mag*, vol. 18, no. 3, pp. 27–33, 1999.

[6] G. H. Kraft, S. S. Fitts, and M. C. Hammond, "Techniques to improve function of the arm and hand in chronic hemiplegia." *Arch Phys Med Rehabil*, vol. 73, no. 3, pp. 220–227, 1992.

[7] T. Bajd, A. Kralj, M. Stefancic, and N. Lavrac, "Use of functional electrical stimulation in the lower extremities of incomplete spinal cord injured patients." *Artif Organs*, vol. 23, no. 5, pp. 403–409, 1999.

[8] E. A. C. Pereira, A. L. Green, D. Nandi, and T. Z. Aziz, "Deep brain stimulation: indications and evidence." *Expert Rev Med Devices*, vol. 4, no. 5, pp. 591–603, 2007.

[9] J. Lian, M. Bikson, C. Sciortino, W. C. Stacey, and D. M. Durand, "Local suppression of epileptiform activity by electrical stimulation in rat hippocampus in vitro." *J Physiol*, vol. 547, no. Pt 2, pp. 427–434, 2003.

[10] K. J. Lee, K. S. Jang, and Y. M. Shon, "Chronic deep brain stimulation of subthalamic and anterior thalamic nuclei for controlling refractory partial epilepsy." *Acta Neurochir Suppl*, vol. 99, pp. 87–91, 2006.

[11] P. Boon, V. De Herdt, K. Vonck, and D. Van Roost, "Clinical experience with vagus nerve stimulation and deep brain stimulation in epilepsy." *Acta Neurochir Suppl*, vol. 97, no. Pt 2, pp. 273–280, 2007.

[12] S. Mayer, L. A. Geddes, J. D. Bourland, and L. Ogborn, "Electrode recovery potential," *Annal. Biomed. Eng.*, vol. 20, pp. 385–394, 1992.

[13] G. A. DeMichele and P. R. Troyk, "Stimulus-resistant neural recording amplifier," in *Proc. IEEE EMBS*, vol. 4, Cancun, Mexico, Sept. 2003, pp. 3329–3332.

[14] J. W. Gnadt, S. D. Echols, A. Yildirim, H. Zhang, and K. Paul, "Spectral cancellation of microstimulation artifact for simultaneuos neural recording *In Situ*," *IEEE Trans. Biomed. Eng.*, vol. 50, no. 10, pp. 1129–1135, Oct. 2003.

[15] Y. Jimbo, N. Kasai, K. Torimitsu, T. Tateno, and H. Robinson, "A system for MEA-based multisite stimulation," *IEEE Trans. Biomed. Eng.*, vol. 50, no. 2, pp. 241–248, Feb. 2003.

[16] S. Hafizovic, F. Heer, T. Ugniwenko, U. Frey, A. Blau, C. Ziegler, and A. Hierlemann, "A cmos-based microelectrode array for interaction with neuronal cultures." *J Neurosci Methods*, 2007.

[17] R. A. Blum, J. D. Ross, E. A. Brown, and S. P. DeWeerth, "An integrated system for simultaneous, multichannel neuronal stimulation and recording," *IEEE Trans. Circuits and Systems I*, vol. 54, no. 12, pp. 2608–2618, December 2007.

[18] R. A. Blum, J. D. Ross, S. K. Das, E. A. Brown, and S. P. DeWeerth, "Models of stimulation artifacts applied to integrated circuit design," in *Proc. of the IEEE Engineering in Medicine and Biology Conference*, San Fransisco, CA, Sept. 2004, pp. 4075–4078.

[19] E. Brown, J. Ross, R. Blum, and S. DeWeerth., "Circuits and methods for artifact elimination." U.S. Patent app. 2007/0178579, 2007.

[20] E. A. Brown, J. D. Ross, R. A. Blum, Y. Nam, B. C. Wheeler, and S. P. DeWeerth, "Stimulus artifact elimination in a multi-electrode system," *IEEE Trans. Biomed. Circuits and Systems*, 2008, accepted for publication.